# Photon Solid Phases in Driven Arrays of Nonlinearly Coupled Cavities

Jiasen Jin, Davide Rossini, and Rosario Fazio
*NEST, Scuola Normale Superiore and Istituto di Nanoscienze-CNR, I-56126 Pisa, Italy*

Martin Leib and Michael J. Hartmann
*Technische Universität München, Physik Department, James-Franck-Strasse, D-85748 Garching, Germany*
(Received 9 February 2013; published 18 April 2013)

We introduce and study the properties of an array of QED cavities coupled by nonlinear elements, in the presence of photon leakage and driven by a coherent source. The nonlinear couplings lead to photon hopping and to nearest-neighbor Kerr terms. By tuning the system parameters, the steady state of the array can exhibit a *photon crystal* associated with a periodic modulation of the photon blockade. In some cases, the crystalline ordering may coexist with phase synchronization. The class of cavity arrays we consider can be built with superconducting circuits of existing technology.

DOI: 10.1103/PhysRevLett.110.163605 PACS numbers: 42.50.Pq, 05.70.Ln, 64.70.Tg, 85.25.Cp

Since its beginning, the study of light-matter interaction in cavity and circuit QED has been providing a very fertile playground to test fundamental questions at the heart of quantum mechanics, together with the realization of very promising implementations of quantum processors [1,2]. The coupling of separate cavities through photon hopping introduces an additional degree of freedom that is receiving increasing interest both theoretically and experimentally.

Cavity arrays, periodic arrangements of neighboring QED cavities, have been introduced [3–5] as prototype systems to study many-body states of light. Their very rich phenomenology arises from the interplay between strong local nonlinearities and photon hopping. In the photon blockade regime, the array enters a Mott insulating phase, where photon number fluctuations are suppressed. In the opposite regime, where the hopping dominates, photons are delocalized through the whole array with long-range superfluid correlations. The phase diagram has been thoroughly studied by a variety of methods, and the locations of the different phases, together with the critical properties of the associated phase transitions, have been determined (see, e.g., the reviews [6–8]).

The properties of cavity arrays resemble in several aspects those of the Bose-Hubbard model [9], as long as particle losses can be ignored. Cavity arrays, however, will naturally operate under nonequilibrium conditions, i.e., subject to unavoidable leakage of photons which are pumped back into the system by an external drive. In this case, the situation may change drastically, and, to a large extent, it is an unexplored territory. Only very recently have the many-body nonequilibrium dynamics of cavity arrays started to be addressed [10–13], thus entering the exciting field of quantum phases and phase transitions in driven quantum open systems [14–19].

Since the very beginning, all the works devoted to cavity arrays studied the case in which adjacent cavities are coupled by photon hopping. In this Letter, we introduce a new class of arrays in which the coupling between cavities is mediated by a nonlinear element or medium. Thanks to the flexibility in the design of the nonlinear coupling elements, these finite-range couplings can appear in the form of cross-Kerr nonlinearities and/or as a correlated photon hopping, leading to a steady-state phase diagram that is a lot richer than the cases which have been considered so far. Here we discuss in particular the appearance of a new phase in cavity arrays, a *photon crystal*, which emerges in the steady-state regime when the array is driven by a coherent homogeneous pump.

A technology that is very well suited for realizing cavity arrays with such features is provided by circuit QED [20], where exceptional light-matter coupling has been demonstrated [21], first experiments with arrays of up to five cavities have been done [22], and great progress towards experiments with lattices of cavities has already been achieved [8].

In the following, we first introduce the model for the cavities with their nonlinear couplings, the external drive, and the unavoidable leakage of photons. We present a possible implementation in an array of circuit-QED cavities that are coupled via a nonlinear element. We then study the steady-state regime by means of a mean-field approach and matrix product operator (MPO) simulations [23]. The scenario that emerges is rather complex, with the appearance of a number of phases and phase instabilities. We focus in particular on the possibility of spatial photon patterns that can emerge. For bipartite lattices the photon blockade is modulated on two different sublattices; furthermore, on increasing the photon hopping it may also coexist with a global coherent state.

*The model.*—The cavity array is sketched in Fig. 1(a). The coupling between the cavities is mediated by a nonlinear element. In the specific implementation in circuit QED, this element is a Josephson nanocircuit. When the coupling between the cavities is realized through the

 

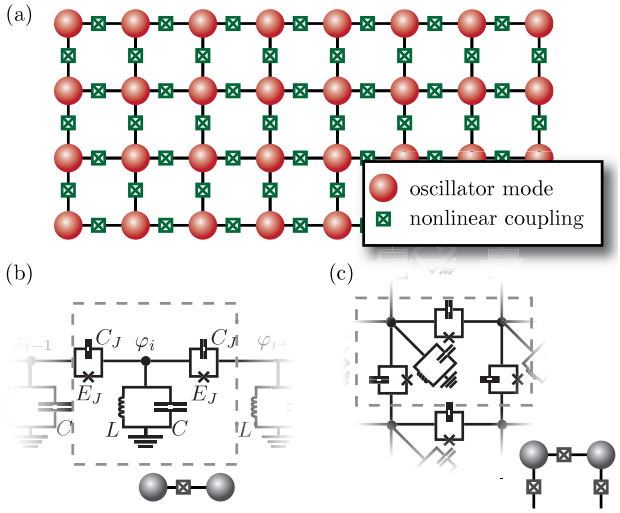


FIG. 1 (color online). (a) An array of QED cavities described by oscillator modes (red circles) that are coupled via nonlinear elements (crossed boxes). (b), (c) Implementation of its building blocks in circuit QED for one- and two-dimensional lattices. The circuit cavities are represented by a $LC$ circuit with capacitance $C$ and inductance $L$ and mutually coupled through a Josephson nanocircuit, with capacitance $C_J$ and Josephson energy $E_J$, that generates the on-site and cross-Kerr terms in Eq. (1). Details of this implementation can be found in Ref. [24]. An alternative approach to cross-Kerr interactions is discussed in Ref. [26].

circuit described in Fig. 1(b), linear tunneling of photons between adjacent cavities can be tuned and even fully suppressed by adjusting the nonlinear coupling circuits to a suitable operating point; see Supplemental Material [24] for details. In this regime the cavities are coupled via a strong cross-Kerr term and further correlated-hopping terms, which can lead to considerable modifications in the phase diagram [25]. Yet there are also more involved approaches involving multiple transmon qubits to realize cross-Kerr interactions in the absence of correlated hoppings [26], see also [27,28]. However, in the regime of parameters we are interested in and where a photon crystal emerges, correlated hopping leads to small quantitative corrections at the expense of complicating considerably the analysis. In the Supplemental Material, we quantify these differences in more detail [24].

Here for simplicity, we concentrate on the salient features of the array in Fig. 1 which are captured by the effective Hamiltonian (in the rotating frame)

$$\mathcal{H} = \sum_i [-\delta a_i^\dagger a_i + \Omega(a_i^\dagger + a_i)] - J\sum_{\langle i,j\rangle}(a_i^\dagger a_j + \text{H.c.}) + U\sum_i n_i(n_i-1) + V\sum_{\langle i,j\rangle} n_i n_j, \quad (1)$$

where the number operator $n_i = a_i^\dagger a_i$ counts the photons in the $i$th cavity [$a_i^\dagger$ ($a_i$) being the creation (annihilation) operator]. The first three terms describe, respectively, the detuning $\delta$ of the cavity mode with respect to the frequency of the pump, the coherent pump with amplitude $\Omega$, and the hopping of photons between neighboring cavities at rate $J$. The last two terms take into account the nonlinearities through the on-site and cross-Kerr terms with the associated energy scales $U$ and $V$, respectively. In the specific case of circuit-QED arrays, the two types of nonlinearities can be realized through the setup of Fig. 1. In order to keep our results as general as possible, we consider the effective model (1) without specifying further the underlying matter-light interaction term.

The dynamics of the array is governed by the master equation

$$\dot\rho = -i[\mathcal{H},\rho] + \frac{\kappa}{2}\sum_i (2a_i\rho a_i^\dagger - n_i\rho - \rho n_i), \quad (2)$$

where $\kappa^{-1}$ is the photon lifetime in each cavity. The model in Eq. (1) together with Eq. (2) encompasses, in some limiting cases, regimes that were already addressed in the literature. The regime of $U\to\infty$ and $J=0$ was considered in Ref. [18], where an antiferromagnetic phase was first predicted in Rydberg atoms. The case of on-site Kerr nonlinearity, i.e., $V=0$, is the only one studied so far in cavity arrays [12]. The model considered here offers a much richer phase diagram. A unique characteristics of the cavity arrays with nonlinear couplings is that the cross-Kerr nonlinearity $V$ can even exceed $U$. By coupling an additional qubit locally to each resonator [29], different ranges of the ratio $V/U$ can be explored. Moreover, in devices where on-chip control lines can be used to locally thread magnetic fields through the loops of the coupling circuits and the additional transmons, the ratios $J/U$ (respectively, $J/V$ and $V/U$) can be tuned on chip. For this reason we will, in the following, consider $U$, $V$, and $J$ as independent.

We first discuss the steady-state phase diagram in the mean-field approximation, which becomes accurate in the limit of arrays with large coordination number $z$. The decoupling in Eq. (1) is performed on the hopping and cross-Kerr terms $z^{-1}\sum_{\langle i,j\rangle} a_i^\dagger a_j \to \langle a_A^\dagger\rangle\sum_{i\in B} a_i + \langle a_B^\dagger\rangle\sum_{j\in A} a_j$ and $z^{-1}\sum_{\langle i,j\rangle} n_i n_j \to \langle n_A\rangle\sum_{i\in B} n_i + \langle n_B\rangle\sum_{j\in A} n_j$, where we assumed a bipartite lattice, $A$ and $B$ being the two sublattices. The mean-field analysis simplifies the dynamics dictated by Eq. (2) to two coupled equations for the two different sublattices. As a function of all the parameters characterizing the system and its dynamics, one gets a very rich behavior in the asymptotic regime which includes steady-state (oscillating) phases, as well as uniform (staggered) configurations. Here we highlight what we think are its most intriguing features. All the couplings will be expressed in units of the photon lifetime $\kappa = 1$.

*Mean-field steady-state diagram.*—Figure 2, where for the moment we set the hopping to zero, shows that, on increasing the cross-Kerr term, the array can reach a steady state in which the photon number is modulated as in a photon crystal, the order parameter being $\Delta n = |\langle n_A\rangle - \langle n_B\rangle|$. Here the area above the green line denotes the

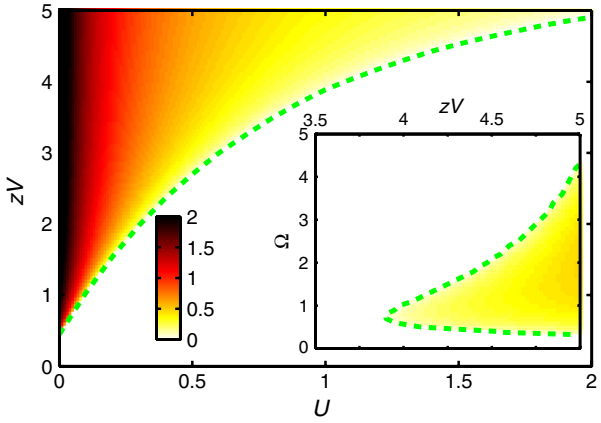


FIG. 2 (color online). Order parameter $\Delta n$ for the photon crystal in the $U$-$V$ plane at zero hopping. If the cross-Kerr term exceeds a critical threshold $V_c$, the steady state is characterized by a staggered order in which $\Delta n \neq 0$. Here we fixed $\Omega = 0.75$ and $\delta = 0$, for which $zV_c \approx 0.44$ at $U = 0$, while $zV_c \approx 5.73$ in the hard-core limit ($U \to \infty$). In the inset, we show $\Delta n$ as a function of $\Omega$ and $V$ at a fixed value of $U = 1$. Here and in the next figure, the color code signals the intensity of the order parameter, while dashed green lines are guides to the eye to locate the phase boundaries.

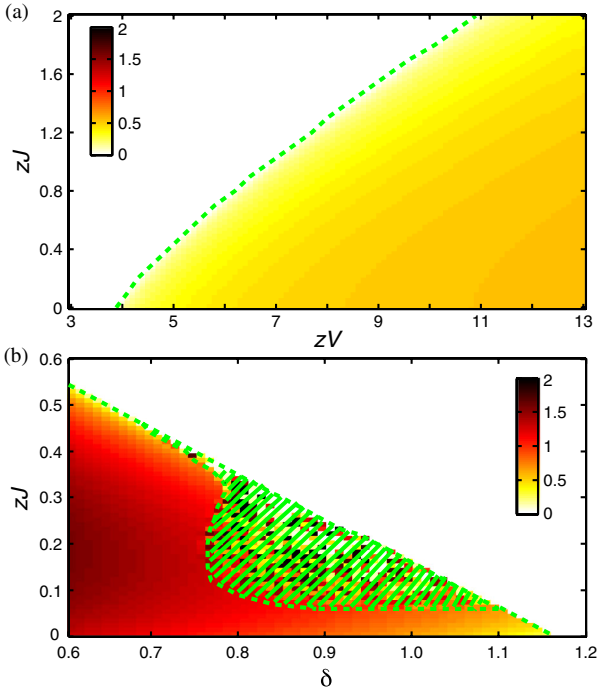


FIG. 3 (color online). Order parameter for the photon crystal at finite hopping. $\Delta n$ is plotted as a function of $J$ and $V$, for $\delta = 0$ and $U = 1$ (a), and as a function of $J$ and $\delta$, for $zV = 0.6$ and $U = 0$ (b). Here we fixed $\Omega = 0.75$. At finite values of the detuning, in addition to the normal (white) and crystalline (colored) phases, an intermediate region (shaded green), characterized by an oscillatory behavior in the asymptotic state, appears. As discussed in the main text, we suggest this last regime may be seen as a nonequilibrium analog of a supersolid.

crystalline phase. In the $U \to \infty$ limit, the transition between the uniform and the crystal phases is located at $zV_c \simeq \gamma_\infty(-2\delta + \sqrt{\gamma_\infty})/4\Omega^2$ with $\gamma_\infty = 4\delta^2 + 8\Omega^2 + 1$, the previous expression holding for small detunings, and coincides with the transition to an antiferromagnetic phase described in Ref. [18]. Note that a lower value of $U$ favors the crystal phase. In the opposite limiting case of $U = 0$, the transition is found at $zV_c \simeq \gamma_0(-2\delta + \sqrt{\gamma_0})/4\Omega^2$ with $\gamma_0 = 4\delta^2 + 1$. We deliberately considered a regime in the parameter space where $V \geq U$, since, as already mentioned, it is a peculiar feature of the cavity arrays proposed here. The transition to the crystal phase is reentrant as a function of the drive (inset in Fig. 2). At very small pumping the density is too low to lead to a photon crystal. Vice versa, it also disappears on increasing $\Omega$, since pumping favors an homogeneous photon arrangement. A similar feature has been observed in the limit $U = \infty$ [18].

If the hopping between photons is switched on, delocalization will suppress the solid phase, and at a critical value of $J$ (which depends on $V$, $U$, $\delta$, and $\Omega$) there is a transition to a normal phase. This is shown in Fig. 3, as a function of the cross-Kerr nonlinearity $V$ [Fig. 3(a)] and of the detuning $\delta$ [Fig. 3(b)]. In Fig. 3(a), we display the case $U = 1$, while at smaller values of $U$ the phase diagram shows a reentrance. Although interesting, further analysis is needed to see if this feature is present only at mean-field level. Yet it does not seem improbable that an increased hopping could facilitate the redistribution of particles into a crystalline order imposed by the interactions. We conclude this discussion by pointing out that, as discussed in Ref. [24], under nonequilibrium conditions it is even possible, although much harder, to realize a crystalline phase at $V = 0$. As a matter of fact, in that case, for some values of the coupling constants, the steady state can be either uniform or crystalline, depending on the initial conditions.

The mean-field phase diagram in the $\delta - J$ plane and for $U = 0$ is depicted in Fig. 3(b). As highlighted in the region between the dashed green lines, for $0.8 \lesssim \delta \lesssim 1.1$, on switching on the photon hopping, a new intermediate phase appears. In this region, even in the long-time limit the state never becomes completely stationary, and there is a residual time dependence of $\langle a \rangle$ with $\langle a_A \rangle \neq \langle a_B \rangle$; i.e., there is an additional time dependence of $\langle a \rangle$ on top of the trivial oscillation with the frequency of the coherent drive that is hidden in our choice of the rotating frame. At the same time, the system shows $\Delta n \neq 0$. In Fig. 4(a), we show the time evolution of the real and imaginary parts of $\langle a \rangle$ for the two sublattices. A closer inspection of the properties of the oscillating phase reveals that the reduced density matrix of a single site (in either of the two sublattices) is a coherent state which evolves periodically in time as shown in Fig. 4(b). There we plotted the Wigner function $W(x, p) = \int \langle x - y|\rho_A|x + y\rangle e^{2ipy} dy$ of one sublattice at a given time, with $x = (a + a^\dagger)/\sqrt{2}$, $p = i(a^\dagger - a)/\sqrt{2}$,

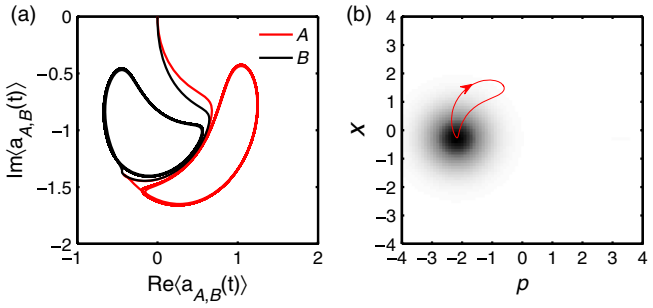


FIG. 4 (color online). (a) Time-dependent traces of the real and imaginary parts of $\langle a \rangle$ for the two sublattices as a function of time in the steady-state regime of the intermediate oscillating phase of Fig. 3(b). (b) The Wigner transform of the reduced single-site density matrix for sublattice $A$ is plotted at a given time in the intermediate oscillating phase of Fig. 3(b). Here we used the same parameters as in Fig. 3(b) and fixed $zJ = 0.2$ and $\delta = 0.9$.

and $|x\rangle$ being an eigenstate of the position operator $x$. Following the analysis performed in Ref. [19], we are led to conclude that in this region the dynamical evolution of the whole array is synchronized separately in the two different sublattices. The contemporary presence of checkerboard ordering and global dynamical phase coherence suggests us to view this intermediate phase as a *nonequilibrium supersolid phase* [30]. The intermediate region extends also at finite-$U$ values, although the coherent state of Fig. 4(b) will be progressively deformed on increasing the on-site repulsion.

*MPO simulations.*—Most of the features we discussed can already be seen in small arrays. To show some examples and to further support the mean-field analysis given above, we here present results that were obtained for linear chains of cavities, $z = 2$, with MPO simulations [12] of the master equation (2), which provide a (numerically) exact description of its nonequilibrium many-body dynamics. Figure 5(a) shows the density-density correlation function $g^{(2)}(i, j) = \langle a_i^\dagger a_j^\dagger a_j a_i \rangle / \langle n_i \rangle \langle n_j \rangle$ for a chain of 20 cavities with $\delta = 0$, $J = 0$, $U = 0.5$, $\Omega = 0.4$, and various values of $V$. One clearly sees that a staggered dependence of the distance $r = |i - j|$, indicating strong density-density correlations, appears for nonzero $V$, whereas for $V = 0$ photons in distinct cavities are uncorrelated ($g^{(2)} = 1$). Figure 5(b) shows $g^{(2)}$ for a chain of 21 cavities with $\delta = 0$, $U = 1$, $V = 1$, $\Omega = 0.4$, and various values of $J$. The spatial range of density-density correlations shrinks with increasing tunneling rate $J$, indicating a crossover to an uncorrelated state. A more quantitative analysis of the decay of correlations with increasing distance is not conclusive for the chain length considered here. A true ordering in the steady state can probably be stabilized only in two dimensions.

*Conclusions.*—In this Letter, we introduced cavity arrays with coupling mediated by nonlinear elements. This opens the way to study a variety of new possibilities, including

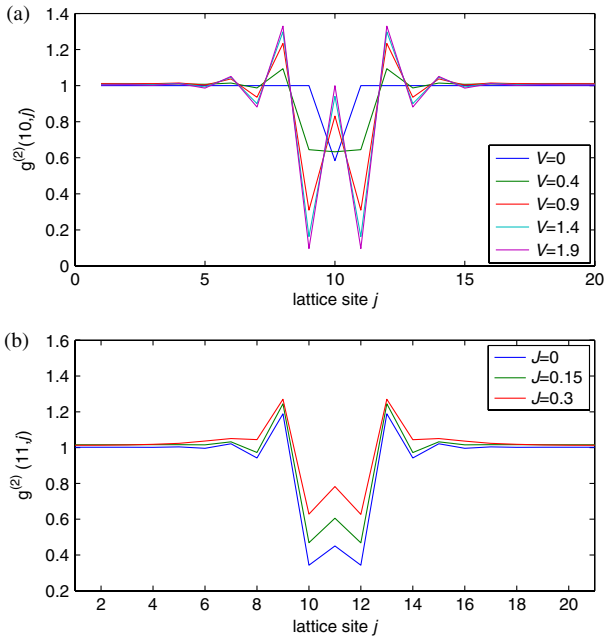


FIG. 5 (color online). MPO results for linear chains of cavities. (a) $g^{(2)}(10, j)$ for $\delta = 0$, $J = 0$, $U = 0.5$, $\Omega = 0.4$, and $V$ as in the legend. (b) $g^{(2)}(11, j)$ for $\delta = 0$, $U = 1$, $V = 1$, $\Omega = 0.4$, and $J$ as in the legend.

correlated photon hopping and finite-range photon blockade. We concentrated on this last point by studying the effect of a cross-Kerr nonlinearity on the steady state and found a very rich phase diagram. A photon solid characterized by a checkerboard ordering of the average photon number appears for a substantial range of the coupling constants. In addition, we see that, for some choice of the parameters, a finite hopping stabilizes a phase where the crystalline ordering coexists with a globally synchronized dynamics of the cavities, suggesting an analogy to a nonequilibrium supersolid. Most of the results presented in this work were obtained in a mean-field approximation. We corroborated the existence of a steady-state solid phase by studying a one-dimensional array by means of a matrix product operator approach. This last analysis confirms that a crystalline ordering of photons can be observed with existing experimental technology.

We acknowledge fruitful discussions with A. Tomadin. This Letter was supported by EU, through Grant Agreement No. 234970-NANOCTM and No. 248629-SOLID, by DFG through the Emmy Noether project HA 5593/1-1 and the CRC 631, and by National Natural Science Foundation of China under Grant No. 11175033.

[1] J. M. Raimond, R. Brune, and S. Haroche, Rev. Mod. Phys. **73**, 565 (2001).
[2] S. M. Girvin, M. H. Devoret, and R. J. Schoelkopf, Phys. Scr. **T137**, 014012 (2009).

[3] M. J. Hartmann, F. G. S. L. Brandão, and M. B. Plenio, Nat. Phys. **2**, 849 (2006).
[4] A. D. Greentree, C. Tahan, J. H. Cole, and L. C. L. Hollenberg, Nat. Phys. **2**, 856 (2006).
[5] D. G. Angelakis, M. F. Santos, and S. Bose, Phys. Rev. A **76**, 031805(R) (2007).
[6] M. J. Hartmann, F. G. S. L. Brandão, and M. B. Plenio, Laser Photon. Rev. **2**, 527 (2008).
[7] A. Tomadin and R. Fazio, J. Opt. Soc. Am. B **27**, A130 (2010).
[8] A. A. Houck, H. E. Türeci, and J. Koch, Nat. Phys. **8**, 292 (2012).
[9] M. P. A. Fisher, P. B. Weichman, G. Grinstein, and D. S. Fisher, Phys. Rev. B **40**, 546 (1989).
[10] I. Carusotto, D. Gerace, H. E. Türeci, S. De Liberato, C. Ciuti, and A. Imamoğlu, Phys. Rev. Lett. **103**, 033601 (2009).
[11] A. Tomadin, V. Giovannetti, R. Fazio, D. Gerace, I. Carusotto, H. E. Türeci, and A. Imamoğlu, Phys. Rev. A **81**, 061801(R) (2010).
[12] M. J. Hartmann, Phys. Rev. Lett. **104**, 113601 (2010).
[13] F. Nissen, S. Schmidt, M. Biondi, G. Blatter, H. E. Türeci, and J. Keeling, Phys. Rev. Lett. **108**, 233603 (2012).
[14] S. Diehl, A. Micheli, A. Kantian, B. Kraus, H. P. Büchler, and P. Zoller, Nat. Phys. **4**, 878 (2008).
[15] S. Diehl, A. Tomadin, A. Micheli, R. Fazio, and P. Zoller, Phys. Rev. Lett. **105**, 015702 (2010).
[16] K. Baumann, C. Guerlin, F. Brennecke, and T. Esslinger, Nature (London) **464**, 1301 (2010).
[17] I. Lesanovsky, B. Olmos, and J. P. Garrahan, Phys. Rev. Lett. **105**, 100603 (2010).
[18] T. E. Lee, H. Häffner, and M. C. Cross, Phys. Rev. A **84**, 031402(R) (2011).
[19] M. Ludwig and F. Marquardt, arXiv:1208.0327.
[20] M. Leib and M. J. Hartmann, New J. Phys. **12**, 093031 (2010).
[21] T. Niemczyk, F. Deppe, H. Huebl, E. P. Menzel, F. Hocke, M. J. Schwarz, J. J. Garcia-Ripoll, D. Zueco, T. Hümmer, E. Solano, A. Marx, and R. Gross, Nat. Phys. **6**, 772 (2010).
[22] E. Lucero, R. Barends, Y. Chen, J. Kelly, M. Mariantoni, A. Megrant, P. O'Malley, D. Sank, A. Vainsencher, J. Wenner, T. White, Y. Yin, A. N. Cleland, and J. M. Martinis, Nat. Phys. **8**, 719 (2012).
[23] M. J. Hartmann, J. Prior, S. R. Clark, and M. B. Plenio, Phys. Rev. Lett. **102**, 057202 (2009).
[24] See Supplemental Material http://link.aps.org/supplemental/10.1103/PhysRevLett.110.163605 for details on the implementation of our proposed circuit-QED setup.
[25] T. Sowiński, O. Dutta, P. Hauke, L. Tagliacozzo, and M. Lewenstein, Phys. Rev. Lett. **108**, 115301 (2012).
[26] Y. Hu, G.-Q. Ge, S. Chen, X.-F. Yang, and Y.-L. Chen, Phys. Rev. A **84**, 012329 (2011).
[27] D. Zueco, J. J. Mazo, E. Solano, and J. J. García-Ripoll, Phys. Rev. B **86**, 024503 (2012).
[28] B. Peropadre, D. Zueco, F. Wulschner, F. Deppe, A. Marx, R. Gross, and J. J. García-Ripoll, Phys. Rev. B **87**, 134504 (2013).
[29] L. Neumeier, M. Leib, and M. J. Hartmann, arXiv:1211.7215.
[30] M. Boninsegni and N. V. Prokof'ev, Rev. Mod. Phys. **84**, 759 (2012).